Published in final edited form as:
Exp Neurol. 2012 January ; 233(1): 581–586. doi:10.1016/j.expneurol.2011.09.031.

External pallidal stimulation improves parkinsonian motor signs and modulates neuronal activity throughout the basal ganglia thalamic network

Jerrold L. Vitek, M.D., Ph.D.[1], **Jianyu Zhang, M.D.**[1], **Takao Hashimoto, M.D.**[2], **Gary Russo, Ph.D.**[3], and **Kenneth B. Baker, PhD**[1]

[1]Department of Neurology, University of Minnesota, Minneapolis, MN, U.S.A

[2]Shinshu University School of Medicine, Matsumoto, Japan

[3]Environmental Protection Agency, Washington, D.C., USA

Abstract

Deep brain stimulation (DBS) of the internal segment of the globus pallidus (GPi) and the subthalamic nucleus (STN) are effective for the treatment of advanced Parkinson's disease (PD). We have shown previously that DBS of the external segment of the globus pallidus (GPe) is associated with improvements in parkinsonian motor signs; however, the mechanism of this effect is not known. In this study, we extend our findings on the effect of STN and GPi DBS on neuronal activity in the basal ganglia thalamic network to include GPe DBS using the MPTP monkey model. Stimulation parameters that improved bradykinesia were associated with changes in the pattern and mean discharge rate of neuronal activity in the GPi, STN, and the pallidal [ventralis lateralis pars oralis (VLo) and ventralis anterior (VA)] and cerebellar [ventralis lateralis posterior pars oralis (VPLo)] receiving areas of the motor thalamus. Population post-stimulation time histograms revealed a complex pattern of stimulation-related inhibition and excitation for GPi and VA/VLo, with a more consistent pattern of inhibition in STN and excitation in VPLo. Mean discharge rate was reduced in GPi and STN and increased in VPLo. Effective GPe DBS also reduced bursting in STN and GPi. These data support the hypothesis that therapeutic DBS activates output from the stimulated structure and changes the temporal pattern of neuronal activity throughout the basal ganglia thalamic network and provide further support for GPe as a potential therapeutic target for DBS in the treatment of PD.

Keywords

deep brain stimulation; globus pallidus; monkey; MPTP (1-methyl-4-phenyl-1,2,3,6-tetrahydropyridine); parkinsonism

Corresponding Author: Jerrold L. Vitek, M.D., Ph.D., Department of Neurology, 12-100 PWB, 516 Delaware St SE, Minneapolis, MN 55455, USA, Phone: 612/624-1903, Fax: 612/625-4195, vitek004@umn.edu.

Introduction

Though highly effective for the treatment of the motor signs of Parkinson's disease (PD), the mechanism underlying deep brain stimulation (DBS) of the internal segment of the globus pallidus (GPi) or the subthalamic nucleus (STN) remains under debate. Currently, two primary mechanistic theories of DBS have been promoted: suppression or activation of the targeted deep brain structure. The suppression theory is derived from several lines of evidence, with the first being the similarity of therapeutic effect on parkinsonian motor signs between surgical ablation or chronic, high-frequency stimulation in the STN, GPi or motor thalamus. Additional, more direct evidence in support of suppression comes from reports of reduced mean discharge rates of neurons at the site of stimulation (Dostrovsky, et al., 2000, Wu, et al., 2001). The activation theory postulates that output from the stimulated structure is increased resulting in a change in the pattern and rate of neuronal activity. This hypothesis receives support from observations that STN DBS increased the mean discharge rate and produced a stereotypical temporal pattern of response in pallidal neurons during stimulation (Hashimoto, et al., 2003). Similar support also comes from the finding of reduced thalamic discharge rates during GPi stimulation in normal monkeys (Anderson, et al., 2003) and in humans with dystonia (Montgomery, 2006). Data from imaging (Jech, et al., 2001, Perlmutter, et al., 2002), microdialysis (Windels, et al., 2000) and modeling studies (McIntyre and Grill, 1999) also support the theory that DBS activates the output of the target subcortical structure. Given our previous findings of improvement in parkinsonian motor signs during GPe stimulation prior to pallidotomy (Vitek, et al., 2004) and the need to evaluate the mechanism of action of DBS further, we implanted a chronic stimulating electrode, similar to that used in our previous nonhuman primate study (Elder, et al., 2005, Hashimoto, et al., 2003), in the GPe of a single monkey rendered parkinsonian with the neurotoxin, 1-methyl-4-phenyl-1,2,3,6-tetrahydropyridine (MPTP). The effect of GPe stimulation on neuronal activity at key nodal points in the basal ganglia thalamic network was examined during therapeutic DBS in the GPe and compared to parameters that did not improve motor signs to delineate the changes that occur in the basal ganglia thalamic network during therapeutic stimulation.

Methods

All surgical and behavioral protocols were approved by the Institutional Animal Care and Use Committee of the Cleveland Clinic Foundation and complied with United States Public Health Service policy on the humane care and use of laboratory animals.

Surgical procedures

A single adult rhesus monkey (*Macaca mulatta*; female, 5.1 kg) was used for this pilot study. Data collection and surgical procedures have been reported previously (Xu, et al., 2008). Briefly, a hemi-parkinsonian syndrome was induced in the left hemi-body by unilateral intracarotid injections of MPTP (0.4–0.65 mg/kg). A separate, aseptic surgical procedure was performed under isoflurane anesthesia to position and secure the cephalic recording chambers. One chamber was oriented in the parasagittal plane to target the GPi, STN and motor thalamus while a second chamber was oriented in the coronal plane to target the GPe.

Pallidal mapping and DBS lead placement

During electrophysiological recording sessions, the awake animal was seated in a primate chair with its head restrained. Glass-insulated platinum-iridium microelectrodes (impedance = 0.5–1.0 MΩ at 1 kHz) were advanced using a hydraulic microdrive mounted on the recording chamber. A map of the pallidum was compiled by classifying neuronal activity using techniques applied during human functional neurosurgery (Vitek, et al., 1998). The

sensorimotor portion of GPe was identified by its characteristic pattern of spontaneous neuronal activity and responses to passive and active movement. Once identified, a scaled down version of the human DBS lead, consisting of four cylindrical metal contacts (each being 0.76 mm diameter, 0.50 mm tall, and separated by 0.5 mm) was implanted in the right GPe as described previously (Elder, et al., 2005) (see Figure 1a). The proximal end was connected to an extension tunneled subcutaneously to a programmable pulse generator (Itrel II, Medtronic, Inc.) implanted between the scapulae. Therapeutic benefit with bipolar stimulation was determined by systematically varying contacts, pulse duration, frequency and voltage as described previously (Hashimoto, et al., 2003). The stimulation parameters that produced the greatest motor benefit without visible side effects were termed “effective” stimulation (Contact $3^{-}/1^{+}$, 135 Hz, 5.5 V), whereas the maximum reduced voltage with no therapeutic benefit was termed “ineffective” (2.0 V).

Electrophysiology measurements of neuronal activity

Once the lead was implanted, spontaneous neuronal activity was recorded in the STN, GPi, and the pallidal [ventralis lateralis pars oralis (VLo)] and cerebellar [ventralis posterolateralis pars oralis (VPLo)] receiving areas of the motor thalamus before, during, and after high frequency (136 Hz) stimulation. In the thalamus, microstimulation was applied at selected intervals (10–40 μA) in 100 ms trains of balanced bipolar pulse pairs (200 μs cathodal pulse, 100 μs gap, 200 μs anodal pulse) at 400 Hz to facilitate distinction of thalamic subnuclei (Vitek, et al., 1996). Neuronal activity was sampled for a minimum of 60 seconds before, during, and after GPe DBS. The amplified and filtered analog signal was sampled with a resolution of 20 μs and digitized. During off-line analysis, stimulation artifacts were removed as described previously (Hashimoto, et al., 2002). Recording sessions occurred over a period of three to four hours.

Behavioral assessments

Bradykinesia was assessed by measuring the time required to retrieve raisins from a 3×3 matrix of 2 cm diameter by 1.2 cm deep wells (Klüverboard) presented to the animal in a standard manner with one forelimb restrained. Total movement time for each trial was defined as the time from initial touch of the first piece of food until contact to the mouth with the last piece across all nine reach and retrieval movements. The left (affected) and right (unaffected) arms were tested individually on 10–15 presentations per session under all three conditions (pre-, peri- and post-stimulation), with the first test of the session alternating between left and right arms on sequential testing days. Statistical comparisons were analyzed using *t*-tests with Bonferroni correction for multiple comparisons. Total movement time data are presented as mean ± standard error.

Data analysis

Post-stimulus time histograms (PSTHs) of activity before and during stimulation were constructed by aligning action potentials with the onset of each stimulus pulse during stimulation or to simulated pulses with the same frequency during spontaneous recordings. Differences in the discharge rate within each bin of the PSTH during stimulation were tested by evaluating the probability that a change in discharge rate within each bin could have occurred by chance compared with the discharge rate predicted by a Poisson distribution with a mean rate of the corresponding bin in the pre-stimulation PSTH ($p \leq 0.05$). Changes in the overall pattern of each PSTH were evaluated by comparing the distribution of bins during stimulation with the distribution before stimulation using a Kolmogorov–Smirnov goodness of fit test. Putative bursts were identified as sequences of interspike intervals (ISI) that were less than the mean ISI of the series using a modified version of the Poisson surprise method (Legendy and Salcman, 1985). These were refined further by calculating the surprise index (SI) of every combination of contiguous spikes and taking the

combination with the highest SI (lowest probability of occurrence). Bursts found in this manner were rejected if they did not consist of a minimum of three spikes or have an SI value of at least three (Wichmann and Soares, 2006), with the spikes being reassigned to the adjacent non-burst period.

Histology

The monkey was deeply anesthetized with pentobarbital and perfused transcardially with normal saline followed by 10% neutral formalin with the DBS lead still in place. The brain was blocked, frozen, and sectioned at 40 μm in the parasagittal plane (anterior to the DBS lead) or coronal plane (posterior to the DBS lead). Figure 1a (left) shows the tissue artifact left by the DBS lead and reveals an implant angle of approximately 35 degrees in the coronal plane. In Figure 1a (right), a sample DBS lead is shown superimposed on the coronal section and aligned over the top of the tissue artifact left by the implanted lead. The figure highlights the position of each of the four contacts of the lead within the pallidal complex, with the distal contact (0) situated within the lateral border of GPi and the remaining three contacts situated partially or wholly within the GPe. Recording sites were confirmed by the linear gliosis associated with microelectrode tracks and the location of small electrolytic lesions (4–10 μA of cathodal DC for 10–20 s) made at pre-determined sites (Figure 1b). Sections were stained alternately with cresyl violet and acetylcholinesterase. VA/VLo, VPLo, and neighboring subnuclei were distinguished using cytoarchitectonic and chemoarchitectonic criteria described previously (Vitek, et al., 1994).

Results

Three hundred and twelve neurons were sampled overall, i.e., 174 during ineffective stimulation only, 186 during effective stimulation only, and 48 under both conditions). During ineffective stimulation, 20 neurons were sampled from the STN, 47 from GPi, 43 from VA/VLo and 64 from VPLo. During effective stimulation, 50 neurons were sampled from the STN, 58 from GPi, 26 from VA/VLo and 52 from VPLo. Figure 1c illustrates the 33% reduction in total movement time observed for the affected arm during therapeutically-effective GPe DBS, $t(42) = 5.52$, $p < 0.001$.

Post-stimulus time histograms revealed changes in spike activity time-locked to each stimulus pulse during effective GPe DBS (Figure 1d). GPi and VLo demonstrated an almost mirror image, biphasic pattern of suppression and excitation. In the GPi, peak suppression occurred at 1.5 ms and 5 ms following the stimulation pulse, with the peaks interrupted by a less robust excitatory peak centered at approximately 4 ms post-stimulation. In the VLo, the dual peaks were excitatory and occurred at approximately 1.2 ms and 4.8 ms, with an intervening trough extending to baseline. Tonic suppression and excitation were observed in the STN and VPLo, respectively. The smoothed running averages for each nodal point are superimposed to the right in Figure 1d to illustrate the relative timing of these activity changes across the network.

Changes in mean discharge rate across the four nodal points are summarized in Figure 1e. Consistent with the PSTH findings, the ANOVA model revealed an effect on mean discharge rate for both the STN ($F_{2,139} = 34.84$, $p < 0.001$) and the GPi ($F_{2,207} = 3.65$, $p = 0.03$). For STN, post-hoc comparisons identified a significant reduction in mean discharge rate (mean ± SD) during effective DBS (9.86 ± 11.70) relative to both the ineffective (19.96 ± 11.81) and OFF condition (28.42 ± 16.32), with the observed difference between ineffective and the OFF condition not reaching significance. For GPi, post-hoc comparisons indicated a significant difference between the effective condition (47.69 ± 29.65) and the ineffective condition (55.33 ± 29.66) and the DBS OFF condition (60.63 ± 28.98), with the difference between the ineffective and OFF condition not achieving significance. Within the

motor thalamus, the model did not show a significant change in mean discharge rate for VLo ($F_{2,135} = 0.12$, $p = 0.88$), however an effect was identified for VPLo ($F_{2,229} = 5.39$, $p = 0.005$). Post-hoc comparisons indicated that the mean discharge rate in the VPLo during the effective condition (21.88 ± 13.59) was elevated relative to both the ineffective and OFF DBS condition (14.99 ± 10.98; 16.34, ± 11.64, respectively), again with no significant difference between the ineffective and DBS OFF condition.

Ineffective and effective GPe DBS were associated with inhibition of 60% or more of the neurons sampled in both the GPi and STN, though a small subpopulation within each structure did exhibit increased activity (see Table). Although the proportion of GPi neurons showing a change in activity did not vary between ineffective and effective stimulation conditions ($\chi^2_{2, N = 105} = 0.18$, $p = 0.92$), a trend was observed in STN towards a greater proportion of its population being inhibited ($\chi^2_{2, N = 70} = 1.80$, $p = 0.35$). In both subnuclei of the thalamus, the transition from ineffective to effective stimulation was associated with an increase in the percentage of the population showing increased activity and associated reduction in the percentage of inhibited neurons. This shift was found to be significant for VA/VLo ($\chi^2_{2, N = 69} = 6.90$, $p = 0.03$), but not VPLo ($\chi^2_{2, N = 116} = 3.48$, $p = 0.18$).

During ineffective stimulation, burst activity was increased in both the STN and GPi compared to DBS OFF, with the proportion of neurons exhibiting bursting behavior being equal to, or outnumbering, neurons that showed a reduced incidence of bursting (see Table). With the transition to effective GPe DBS, this condition reversed, as a greater proportion of neurons in both the STN ($\chi^2_{2, N = 70} = 9.05$, $p < 0.01$) and GPi ($\chi^2_{2,N = 105} = 22.84$, $p < 0.01$) showed reduced burst activity. In the motor thalamus, approximately one quarter of the population sampled showed an increase in bursting incidence, with a smaller subpopulation exhibiting reduced burst activity; however, there was no significant change in this proportion for either VA/VLo ($\chi^2_{2, N = 69} = 1.43$, $p = 0.49$) or VPLo ($\chi^2_{2, N = 116} = 0.28$, $p = 0.87$) between the ineffective and effective conditions.

Discussion

Acute stimulation in the GPe improves bradykinesia in the parkinsonian monkey coincident with significant changes in pattern, mean discharge rate, and the incidence of bursting activity of neurons across the basal ganglia thalamic circuit. Changes in the pattern of neuronal activity were present independent of an associated change in the mean discharge rate, suggesting that improvements in motor behavior may relate more to changes in the temporal pattern of neuronal activity across the basal ganglia thalamic circuit. This is emphasized by the fact that STN stimulation increases mean discharge rates in GPi, while GPe DBS decreases them, while both GPe and STN DBS alter the temporal pattern of neuronal activity in GPi (Hashimoto, et al., 2003).

The present observation of suppression of neuronal activity in the STN and GPi during GPe stimulation is consistent with the hypothesis that DBS activates output from the stimulated site and modifies neuronal activity throughout the basal ganglia thalamic circuit. Suppression of STN activity and the latency of the onset of inhibition are consistent with activation of the inhibitory projections between the GPe and STN. The pattern of response in GPi neurons resembles that reported previously during STN stimulation where a period of activation followed by suppression and another period of activation was observed (Hashimoto, et al., 2003). In the case of GPe DBS however, this pattern was reversed with a period of suppression followed by a small period of activation and larger period of suppression. Potential pathways mediating GPi suppression during GPe stimulation include activation of the “direct pathway” as it passes through the GPe in route to the GPi, activation of GPe axonal projections to the GPi and/or removal of STN excitatory input to GPi via

inhibition of STN neurons. Prior work by Asdourian et al., conducted in a rodent animal model, also supports that activation of the direct pathway can occur during GPe stimulation (Asdourian, et al., 1991). In that study, the authors observed that acute electrical stimulation of the rodent homologue of the GPe in primates had persistent effects on motor activity following kainic acid (fiber-sparing) lesions of GP consistent with activation of striatopallidal fibers passing through the GP, i.e., direct pathway. Thus, although we are not able to determine the precise mechanism and/or pathways that mediate the observed pattern in this study since the pattern observed in the PSTH represents a sum of activity patterns over a population of neurons averaged over multiple time periods, we can make some testable hypotheses. We would hypothesize that the initial inhibition is mediated by a combination of activation of fibers of the direct pathway together with activation of axonal projections from the GPe to GPi. The period of activation observed between periods of suppression could occur as a result of superimposed excitation of glutamatergic axonal collaterals from the STN to GPe that branch to the GPi. Given the time frame for the second wave of suppression observed at 5 ms, we would propose this occurs as a result of GPe activation producing suppression of STN excitatory projections to the GPi.

In the motor thalamus, we observed clear differences in the type and pattern of changes between the VLo and VPLo. Although the mean discharge rate did not change significantly in the VLo, there was a distinct change in the pattern of neuronal activity that appeared to mirror the changes in the Gpi pattern although shifted in time. The changes in VLo likely occur as a direct result of the changes in GPi neurons projecting to the VLo. Differences in the timing of excitation phases in VLo to suppression in GPi are likely shifted due to the continuous stimulation paradigm used in this study. Additional influences on VLo activity may also occur from other pathways projecting to the VLo that are influenced by stimulation in the GPe, including the substantia nigra pars reticulata, reticular thalamus and pedunculopontine nucleus.

In contrast to the oscillatory pattern observed in VLo, VPLo demonstrated a consistent and tonic pattern of activation during effective DBS. Although the mean discharge rate in VPLo was increased significantly during effective stimulation, there was not a significant change in the relative number of cells that increased their firing rate during effective versus ineffective stimulation. This would support the hypothesis that during effective stimulation the same population of neurons was affected, but more intensely, i.e., increased voltage produced a greater increase in mean discharge rate in the affected neuronal population, but the affected population did not change. In contrast, there was a significant increase in the number of neurons in VLo that increased their discharge rate during effective stimulation despite only a trend towards increased mean discharge rate. This may be explained in part by the sample size and the fact that the increase was not sustained during the entire interpulse interval.

The present data are consistent with our previous report of an increase in GPi mean discharge rate and regularization of the pattern of GPi neuronal activity during STN stimulation in the MPTP monkey model of PD (Hashimoto, et al., 2003). These data are also consistent with previous observations from a variety of studies supporting an increase in output from the stimulated site based upon microdialysis (Windels, et al., 2000), electrophysiology (Anderson, et al., 2003), imaging (Perlmutter, et al., 2002) and clinical data (Yelnik, et al., 2000) as well as theoretical models (McIntyre and Grill, 1999). The present observation of improvement in bradykinesia during GPe stimulation in the monkey is also consistent with observations in PD patients undergoing GPe stimulation (Vitek, et al., 2004, Yelnik, et al., 2000).

There are several limitations to this study. First, although the results were highly consistent and statistically significant they are from one animal and the data need to be substantiated with another subject. Other limitations are that we focused on bradykinesia and did not examine the specific timing of neuronal activity changes in the pallidothalamocortical network, i.e., changes that may occur over time following each stimulus pulse or between stimulation spikes, nor changes in one cell relative to another within and across nodal points. However, using the method of deriving PSTHs, we were able to observe the average changes over time. Although we did not examine the relative role of the direct versus indirect pathway and precise mechanisms in mediating the changes observed in this initial study, future work towards answering these questions will be important: 1) to determine the specific pathophysiological changes that mediate individual parkinsonian motor signs and 2) to optimize the application of DBS to treat these motor signs.

Conclusions

High-frequency stimulation in the GPe improves bradykinesia and elicits a combination of changes in pattern and rate of neuronal activity that occur throughout nodal points in the basal ganglia thalamic network. These changes occur predominately at stimulation parameters that improve parkinsonian motor signs and are likely explained by activation of inhibitory fibers from the striatum and/or external pallidum during stimulation. GPe may provide an alternative target for DBS that is not complicated by the spread of current into the internal capsule and evokes a different set of changes in pattern and rate throughout the pallidothalamic network than either STN or GPi DBS which could potentially provide greater benefit to selected subgroups of PD patients.

Acknowledgments

This work was supported by National Institutes of Health Grant R01NS37019.

References

1. Anderson ME, Postupna N, Ruffo M. Effects of high-frequency stimulation in the internal globus pallidus on the activity of thalamic neurons in the awake monkey. J Neurophysiol. 2003; 89:1150–1160. [PubMed: 12574488]
2. Asdourian D, Lentz SI, Kelland MD. Motor effects of globus pallidus stimulation in the rat: lesions to corticofugal fibers block the motor effects. Behav Brain Res. 1991; 44:185–193. [PubMed: 1751009]
3. Dostrovsky JO, Levy R, Wu JP, Hutchison WD, Tasker RR, Lozano AM. Microstimulation-induced inhibition of neuronal firing in human globus pallidus. J Neurophysiol. 2000; 84:570–574. [PubMed: 10899228]
4. Elder CM, Hashimoto T, Zhang J, Vitek JL. Chronic implantation of deep brain stimulation leads in animal models of neurological disorders. J Neurosci Methods. 2005; 142:11–16. [PubMed: 15652612]
5. Hashimoto T, Elder C, Vitek J. A template subtraction method for stimulus artifact removal in high-frequency deep brain stimulation. J Neurosci Methods. 2002; 113:181–186. [PubMed: 11772439]
6. Hashimoto T, Elder CM, Okun MS, Patrick SK, Vitek JL. Stimulation of the Subthalamic Nucleus Changes the Firing Pattern of Pallidal Neurons. Journal of Neuroscience. 2003; 23:1916–1923. [PubMed: 12629196]
7. Jech R, Urgosik D, Tintera J, Nebuzelsky A, Krasensky J, Liscak R, Roth J, Ruzicka E. Functional magnetic resonance imaging during deep brain stimulation: a pilot study in four patients with Parkinson's disease. Mov Disord. 2001; 16:1126–1132. [PubMed: 11748747]
8. Legendy CR, Salcman M. Bursts and recurrences of bursts in the spike trains of spontaneously active striate cortex neurons. J Neurophysiol. 1985; 53:926–939. [PubMed: 3998798]

9. McIntyre CC, Grill WM. Excitation of central nervous system neurons by nonuniform electric fields. Biophys J. 1999; 76:878–888. [PubMed: 9929489]
10. Montgomery EB Jr. Effects of GPi stimulation on human thalamic neuronal activity. Clin Neurophysiol. 2006; 117:2691–2702. [PubMed: 17029953]
11. Perlmutter JS, Mink JW, Bastian AJ, Zackowski K, Hershey T, Miyawaki E, Koller W, Videen TO. Blood flow responses to deep brain stimulation of thalamus. Neurology. 2002; 58:1388–1394. [PubMed: 12011286]
12. Vitek JL, Ashe J, DeLong MR, Alexander GE. Physiologic properties and somatotopic organization of the primate motor thalamus. J Neurophysiol. 1994; 71:1498–1513. [PubMed: 8035231]
13. Vitek JL, Ashe J, DeLong MR, Kaneoke Y. Microstimulation of primate motor thalamus: Somatotopic organization and differential distribution of evoked motor responses among subnuclei. J Neurophysiol. 1996; 75:2486–2495. [PubMed: 8793758]
14. Vitek JL, Bakay RA, Hashimoto T, Kaneoke Y, Mewes K, Zhang JY, Rye D, Starr P, Baron M, Turner R, DeLong MR. Microelectrode-guided pallidotomy: technical approach and its application in medically intractable Parkinson's disease. J Neurosurg. 1998; 88:1027–1043. [PubMed: 9609298]
15. Vitek JL, Hashimoto T, Peoples J, DeLong MR, Bakay RA. Acute stimulation in the external segment of the globus pallidus improves parkinsonian motor signs. Mov Disord. 2004; 19:907–915. [PubMed: 15300655]
16. Wichmann T, Soares J. Neuronal firing before and after burst discharges in the monkey basal ganglia is predictably patterned in the normal state and altered in parkinsonism. J Neurophysiol. 2006; 95:2120–2133. [PubMed: 16371459]
17. Windels F, Bruet N, Poupard A, Urbain N, Chouvet G, Feuerstein C, Savasta M. Effects of high frequency stimulation of subthalamic nucleus on extracellular glutamate and GABA in substantia nigra and globus pallidus in the normal rat. European Journal of Neuroscience. 2000; 12:4141–4146. [PubMed: 11069610]
18. Wu YR, Levy R, Ashby P, Tasker RR, Dostrovsky JO. Does stimulation of the GPi control dyskinesia by activating inhibitory axons? Movement Disorders. 2001; 16:208–216. [PubMed: 11295772]
19. Xu W, Russo GS, Hashimoto T, Zhang J, Vitek JL. Subthalamic nucleus stimulation modulates thalamic neuronal activity. J Neurosci. 2008; 28:11916–11924. [PubMed: 19005057]
20. Yelnik J, Damier P, Bejjani BP, Francois C, Gervais D, Dormont D, Arnulf I, AMB, Cornu P, Pidoux B, Agid Y. Functional mapping of the human globus pallidus: contrasting effect of stimulation in the internal and external pallidum in Parkinson's disease. Neuroscience. 2000; 101:77–87. [PubMed: 11068138]

Highlights

- GPe stimulation improves motor signs in the MPTP monkey model of PD.
- GPe stimulation suppresses neuronal activity in STN and GPi.
- Gpe stimulation changes the pattern of neuronal activity in GPi and VLo.
- Stimulation in GPe increases mean discharge rates in VPLo.

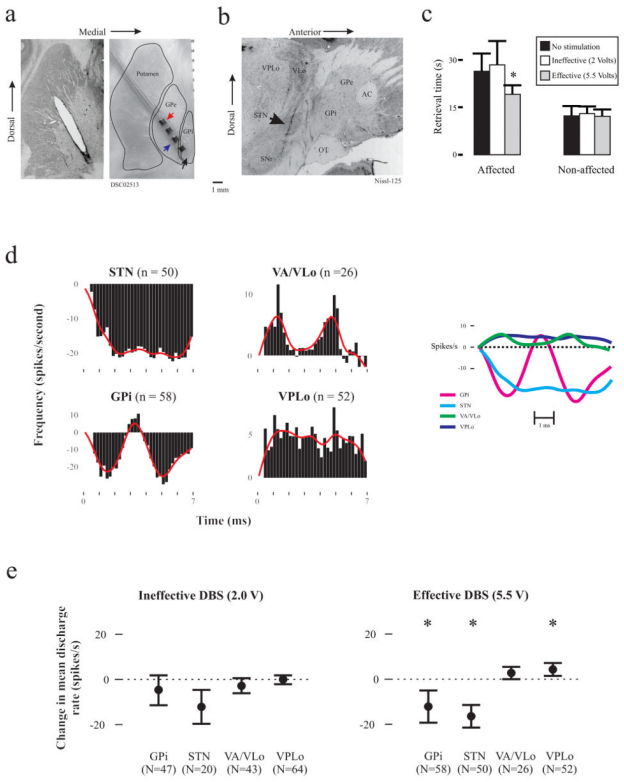

Fig 1.

a. Histological reconstructions of DBS lead placement within the pallidal complex. Left: Coronal section showing the tissue artifact within the striatum and pallidal complex. Right: Gross histological section with a scaled-down DBS lead superimposed on the tissue artifact that remained after its post-mortem removal, illustrating its course and position relative to the pallidum. Red and blue arrows note the relative location of the cathode and anode used in the current study, respectively. **b**. Sample sagittal section revealing the location of recording tracks, including at least one track through the STN (arrow). **c.** Bar graph illustrating the effect of GPe DBS on motor performance. Reach and retrieval times for the affected (left) and non-affected (right) upper extremity during the DBS OFF condition as well as DBS at ineffective, non-therapeutic (2 V) and effective, therapeutic (5.5 V) voltage settings. * Compared to control: $t(42) = 5.52$, $p < 0.001$ **d.** Population post-stimulation time histograms (PSTHs) during effective GPe DBS, where the continuous line represents a smoothed running average of the PSTH data. On the right, each PSTH smoothed running average is superimposed to allow for comparison across the four nodal points examined. For all figures, the x-axis is the time in ms after the stimulation pulse, while the y-axis represents spikes per second (bin width = 0.2 ms). **e.** Change in mean discharge rate during GPe DBS ("on" minus "off") for GPi, STN, VPLo and VA/VLo neurons during effective (5.5 V) and ineffective (2.0 V) stimulation (* $p < 0.05$). VA, ventralis anterior; AC, anterior commissure; OT, optic tract; SNr, substantial nigra pars reticulata.

Table 1

Incidence (%) of rate and bursting changes during Gpe DBS

RATE				
	Excitation	**Inhibition**	**No Change**	
GPi				
Effective	22	66	12	--
Ineffective	25	62	13	--
STN				
Effective	6	76	18	--
Ineffective	10	60	30	--
VA/VLo				
Effective	50	15	35	***p*** **< 0.05**
Ineffective	21	35	44	--
VPLo				
Effective	48	19	33	--
Ineffective	31	24	45	--
BURSTING				
	Increased	**Decreased**	**No Change**	
GPi				
Effective	15	76	9	***p*** **< 0.05**
Ineffective	53	30	17	--
STN				
Effective	10	48	42	***p*** **< 0.05**
Ineffective	40	40	20	--
VA/VLo				
Effective	19	15	66	--
Ineffective	30	19	51	--
VPLo				
Effective	23	12	65	--
Ineffective	27	9	64	--